Vol. 585: 113–121, 2017
https://doi.org/10.3354/meps12395

MARINE ECOLOGY PROGRESS SERIES
Mar Ecol Prog Ser

Published December 27

Baited Remote Underwater Video surveys undercount sharks at high densities: insights from full-spherical camera technologies

James P. Kilfoil[1,*], Aaron J. Wirsing[2], Matthew D. Campbell[3], Jeremy J. Kiszka[1], Kirk R. Gastrich[1], Michael R. Heithaus[1], Yuying Zhang[1], Mark E. Bond[1]

[1]Department of Biological Sciences, Florida International University, North Miami, FL 33181, USA
[2]School of Environmental and Forest Sciences, University of Washington, Seattle, WA 98195, USA
[3]National Marine Fisheries Service, Southeast Fisheries Science Center, Mississippi Laboratories, Pascagoula, MS 39567, USA

ABSTRACT: Video surveys are an essential tool for monitoring marine communities. Their use to study elasmobranch populations has dramatically increased over the last decade. However, the restricted field-of-view (FOV) of traditional cameras in these surveys may bias abundance estimates in a number of ways, including saturation at high densities and low detection probability for rare or cryptic species. This study investigated these potential biases using newly developed full-spherical (FS) camera technology. A comparison of 35 Baited Remote Underwater Video surveys (BRUVs), using both FS and traditional cameras, was conducted from July to August 2016 in shallow waters (0.4 to 8.5 m) of Tetiaroa, French Polynesia. Both blacktip reef *Carcharhinus melanopterus* and sicklefin lemon sharks *Negaprion acutidens* were quantified from traditional cameras using MaxN and MeanCount methods. These estimates were then regressed against FS cameras counts, which were assumed to more accurately represent site abundance, to test for gear saturation. Detection probabilities of the traditional and FS cameras were assessed using a Bayesian binomial model, with uninformed-uniform priors. Results indicated a significant effect of gear saturation for standard BRUVs as counts on FS cameras increased, regardless of the metric used. Furthermore, traditional cameras had a significantly lower detection probability (mean ± 2 SD: 69.88 ± 0.008 %) than FS cameras (81.20 ± 0.007 %). Our findings show that traditional cameras are unlikely to adequately discriminate differences in shark relative abundance at high densities. Therefore, standard BRUV techniques that use restricted FOV cameras are likely limited in their ability to provide accurate information to managers once populations have reached particular thresholds of abundance.

KEY WORDS: 360° cameras · Detectability · Elasmobranchs · Monitoring · Video surveys

INTRODUCTION

Over the last few decades many elasmobranch populations have experienced dramatic population declines (Ferretti et al. 2010, Worm et al. 2013, Dulvy et al. 2014). Though the magnitude of these declines varies considerably across species and ecosystems, an increasing number of shark and ray populations are in need of conservation and management actions (Dulvy et al. 2014, 2017). Effective elasmobranch conservation efforts rely on our ability to assess spatial and temporal variation in the abundance of populations, which is critical for identifying conservation priorities and assessing the progress of current recovery efforts (Cortés et al. 2015). Unfortunately, nearly half of all known elasmobranch species

*Corresponding author: jkilf001@fiu.edu

remains 'Data Deficient' (Dulvy et al. 2014), posing a significant obstacle to their future conservation. Traditionally, elasmobranch population data have been gathered through a combination of fisheries-independent and dependent sources, employing gears such as longlines, gill nets, and trawls from which catch per unit of effort (CPUE) data is used to estimate relative abundance. Though useful tools, these methods have limitations, including an inability to survey high complexity habitats such as coral reefs (Williams et al. 2010), high levels of physiological stress (Mandelman & Skomal 2009, Kneebone et al. 2013, Gallagher et al. 2014) and increased post-release mortality for a number of species (Morgan & Carlson 2010, Dapp et al. 2017, Kilfoil et al. 2017). Video surveys have emerged as a potential way to address the deficiencies of traditional sampling methods, while also reducing current data gaps.

Video surveys have been increasingly used to assess the diversity and relative abundance of marine species across the globe (Whitmarsh et al. 2017). They are particularly suitable for the study of elasmobranchs because of their non-extractive nature (Cappo et al. 2007) and ability to sample previously 'inaccessible' environments (Whitmarsh et al. 2017). Though gathering data on sex, size, and individual recapture rates is more difficult with these methods than with traditional fishing gears, they provide a number of advantages including a permanent record of the data (Harvey et al. 2013), insights on species behavior and habitat use (Langlois et al. 2010, Bacheler et al. 2013), and reduced issues with size (Wells et al. 2008) and species (Bacheler et al. 2013) selectivity to fishing gears. For elasmobranchs, one of the most common video survey approaches is the use of Baited Remote Underwater Video surveys (BRUVs; e.g. Bond et al. 2012, Clarke et al. 2012, Santana-Garcon et al. 2014). A BRUV consists of a single, aka. mono, camera deployed behind a bait source, and provides stationary point counts for species of interest that swim into the camera's field-of-view (FOV) over a specified duration. To eliminate multiple counting of fishes swimming in and out of the FOV, 1 of 2 relative abundance metrics are often used: MaxN (Ellis & DeMartini 1995) or MeanCount (Conn 2011). MaxN is defined as the maximum number of a species observed on any frame of a video (Ellis & DeMartini 1995), whereas MeanCount provides an average count of the species observed over a sub-sample of video frames (Conn 2011). Although widely used (e.g. Willis & Babcock 2000, Stoner et al. 2008, Schobernd et al. 2014), these metrics have recently been criticized due to their inability to account for non-uniform spatial distributions of species around the camera (Campbell et al. 2015), and they may also result in biased estimates in high density environments because of issues stemming from FOV saturation.

A fundamental assumption required to use indices of relative abundance (I) to monitor populations is that they be linearly related to the true site abundance (N) given a constant catchability coefficient (q):

$$I = qN \quad (1)$$

If this assumption is violated or invalid, the metric of relative abundance may overestimate (hyperstable) or underestimate (hyperdepleted) abundance, resulting in imprecise indices which in turn will compromise the integrity of management decisions (Cooke & Beddington 1984). In the case of video surveys, simulation work has shown that this fundamental assumption may not hold true for teleost fishes due to limited FOVs failing to capture the non-uniform spatial distribution of fishes around the camera (Campbell et al. 2015). However, no work has addressed this issue specifically for elasmobranchs. For large-bodied fishes, including many elasmobranchs, a further hindrance may be the saturation of cameras in high density environments. Under these conditions, cameras may not be able to detect increases in abundance beyond some maximum observable threshold, resulting in a hyperstable relationship whereby catchability decreases as true site abundance increases. Furthermore, cameras with a restricted FOV may reduce detection probabilities for elasmobranchs, which will in turn impact standardized indices of relative abundance through inflated zero counts (Campbell et al. 2015, Cortés et al. 2015). Given that one of the greatest challenges currently facing elasmobranch stock assessments is generating accurate and precise indices of relative abundance (Cortés et al. 2015), these issues must be resolved if video surveys are to be used to monitor these populations. Recently developed full-spherical (FS) underwater video platforms may offer a means to test these concerns regarding the use of video surveys to monitor elasmobranchs. In this paper, we used this newly developed technology to conduct the first FS video survey of elasmobranchs. Specifically, our objectives were to determine (1) if the catchability (i.e. q) of reduced FOV (mono) cameras derived from estimates of MaxN and MeanCount is constant across a range of site densities as estimated from FS cameras; and (2) the detection probability for mono and FS cameras.

MATERIALS AND METHODS

Data collection

All video data were collected from 17 July to 8 August 2016, in Tetiaroa; a small French Polynesian atoll in the Society Archipelago. Sampling locations were chosen haphazardly throughout the atoll's inner lagoon at depths ranging from 0.4 to 8.5 m. All deployments were conducted on sandy sediment, with a single BRUV deployed at any one time. At each sampling site, a small aluminum frame was deployed with approximately 1 kg of crushed sardines inside a wire mesh container that was attached to a bait arm (Fig. 1). The aluminum frame (hereafter referred to as BRUV^{fs}), was equipped with both a single GoPro camera (hereafter referred to as the 'mono camera') as well as 6 GoPro cameras mounted above the frame in a GoPro Freedom360 (F360)^{TM} housing (collectively referred to as a FS camera). To correct for light refraction underwater, dome port lenses were applied to all cameras in the F360. Although mono and FS cameras were set at 30 frames s^{-1}, FS cameras had additional setting requirements needed to synchronize and stitch FS videos correctly (see the Appendix and an example 360° video in the Supplement at www.int-res.com/articles/suppl/m585p113_supp/). To ensure units were not deployed on top of live reef habitat, they were set by snorkelers who could visually confirm the location and orientation of the frame for each deployment. Once settled on the sea floor, cameras soaked for approximately 60 min. Following deployment, depth and GPS coordinates of each site were recorded. Following video synchronization and stitching of video files, FS and mono videos were reviewed and annotated by trained, independent observers who estimated MaxN as well as MeanCount (derived from images sequenced every 10 s) beginning once the frame was securely on the sea floor. To reduce issues with observer bias, MaxN and MeanCount were estimated by different individuals for each video.

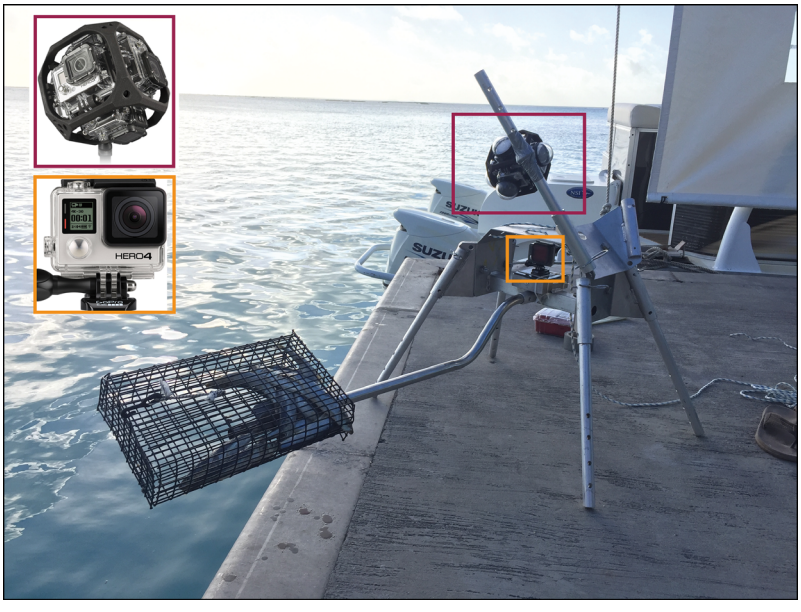

Fig. 1. Baited Remote Underwater Video full-spherical (BRUV^{fs}) array deployed in Tetiaroa, French Polynesia (17 July to 8 August 2017). Red inset depicts GoPro F360 mounting used to later generate full-spherical videos, with its location on the BRUV^{fs} highlighted with a red square. Orange inset depicts the single Hero4 GoPro used as the mono camera comparison, with its location on the BRUV^{fs} highlighted with a corresponding orange square

Relationship between video counts and site abundance

Two metrics were used to enumerate elasmobranchs from video data: MaxN and MeanCount. To examine the relationship between counts derived from mono cameras and site density, we assumed that the corresponding estimates derived from FS cameras (both MaxN and MeanCount) represented a site's true abundance (as the abundance of each site could not be independently estimated), and that the volume of area sampled did not change between sites. Given these assumptions, and substituting for Eq. (1):

$$\mathrm{Mono}_{\mathrm{Est}} = q \times \mathrm{FS}_{\mathrm{Est}} \quad (2.1)$$

which, when rearranged, gives:

$$q = (\mathrm{Mono}_{\mathrm{Est}})/(\mathrm{FS}_{\mathrm{Est}}) \quad (2.2)$$

where q denotes the catchability coefficient, $\mathrm{Mono}_{\mathrm{Est}}$ represents the count derived from the mono camera, and $\mathrm{FS}_{\mathrm{Est}}$ is the FS camera estimate. Under the assumption that estimates derived from mono cameras exhibit a consistent linear relationship to true site abundance over a range of site densities, we would expect q to remain relatively constant. To test this assumption, q of each estimate was plotted against the FS estimate, and a linear model was developed to test for any relationship between q (response variable) and site abundance (predictor variable) using the base 'lm' function in R (R Core Team 2015).

Detection probability

To estimate the detection probability for both mono and FS cameras, we examined the probability of detection at 2 scales: (1) a single image, and (2) the video as a whole. At the single image scale, detection histories for each camera type were categorized for every image as either both detected an elasmobranch (1,1), the mono camera detected an elasmobranch whereas the FS camera did not (1,0), the mono camera did not detect an elasmobranch but the FS camera did (0,1), or neither camera detected an elasmobranch (0,0). For each image, a 'true presence' was determined based on these catch histories, with (0,0) indicating absence and any other indicating presence. For each video, data were aggregated to elucidate the total number of images, the number of images in which a shark was present, the number of images in which a shark was detected by the FS camera, and the number of images in which a shark was detected by the mono camera. Detection probability for each camera was then estimated within a Bayesian framework using the 'rjags' package (Plummer 2013) in R (R Core Team 2015). Under this Bayesian framework, rather than assuming that a catch history of (0,0) is always indicative of true absence, we modeled the probability of occurrence as a Bernoulli process with an uninformed-uniform prior between 0 and 1. The detection probabilities of the mono and FS cameras were modeled using a binomial distribution, also using uninformed-uniform priors between 0 and 1. Models were run for 100 000 iterations, with the first 10 000 iterations disregarded. To examine detection probability for the video as a whole, similar catch histories were developed as previously described (e.g. [0,1] indicates a shark was observed on the FS but not on the mono camera), but from the entire video rather than an individual image. Again, a species was considered absent only for a catch history of (0,0). The probability of a false negative (reporting a catch of 0, when it was truly present) was then calculated for both camera types and all observed elasmobranch species by summing their respective catch histories, divided by the total number of videos in which the species was present.

RESULTS

We deployed the BRUV^{fs} platform 43 times at a variety of locations throughout Tetiaroa, French Polynesia. During those deployments, turbidity ranged from a scale of 1 (clear) to 5 (visibility < 1 m). Eight deployments had camera issues and or short recording times (<40 min) and were thus excluded from analyses, resulting in a total of 35 samples. Although a large diversity of reef fish species was observed on the collected videos, only 2 shark species were detected: blacktip reef *Carcharhinus melanopterus* and sicklefin lemon sharks *Negaprion acutidens*. Accordingly, all MaxN (maximum count on any 1 frame) analyses pertaining to video data focused on these 2 species separately. However, resulting sequenced images had a number of partial sharks present (i.e. only snout or portion of the caudal fin visible), which reduced the ability of observers to distinguish between these 2 species. To account for this limitation, all counts of shark species present on a particular image were aggregated for subsequent analyses pertaining to MeanCount (average count over a sub-sample of frames). Slight differences in recording times between sets resulted in small variations in MeanCount sample sizes (mean ± SD: 395.49 ± 139.01). Average MaxN estimates from mono cameras for blacktip reef (5.06 ± 4.17) and sicklefin lemons (1.94 ± 2.42) were lower than those provided by FS cameras (blacktip reef: 6.62 ± 6.04; sicklefin lemon: 2.03 ± 2.64). Similarly, MeanCount estimates were lower on mono cameras (1.40 ± 1.65) than FS cameras (3.25 ± 3.69). Furthermore, a higher rate of images with zero counts was observed on the mono camera (n = 3930) compared to the FS camera (n = 2120).

Relationship between catchability and true site abundance

FS cameras provided a substantial increase in FOV, which often resulted in higher shark counts compared to the standard mono camera (Fig. 2). Regardless of the relative abundance metric used, catchability of mono cameras decreased linearly as abundance on the FS camera increased (Fig. 3). For estimates of MaxN, this relationship held true for both sicklefin lemon and blacktip reef sharks ($p < 0.05$ for both species; Fig. 3A). However, for sicklefin lemon sharks, which were detected in lower abundances, the negative correlation between catchability and site abundance was heavily influenced by 2 data points, with all others showing no relationship. Consistent with these findings, catchability derived from MeanCount estimates also showed a significant negative relationship with site abundance ($p < 0.001$; Fig. 3B).

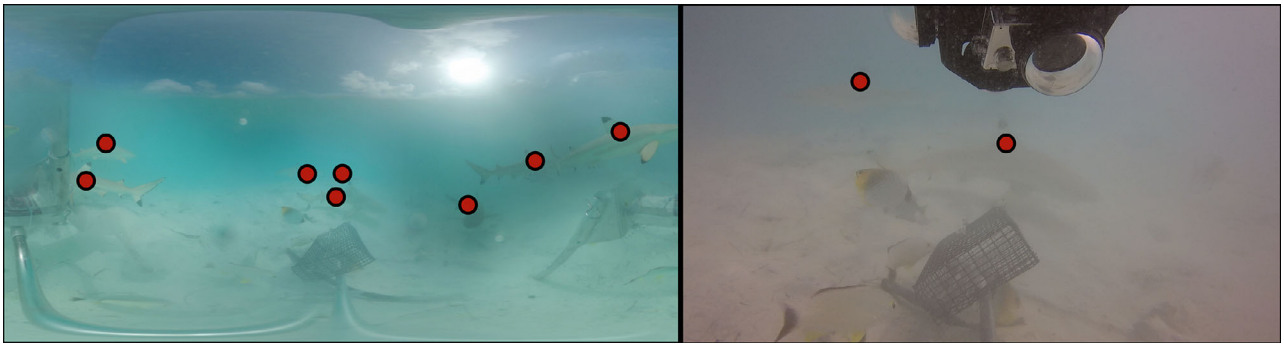

Fig. 2. Still images extracted from stitched full-spherical (left panel) and mono (right panel) Baited Remote Underwater Video (BRUV) deployments in Tetiaroa, French Polynesia (August 2016). Red dots: elasmobranch individuals that could be identified (left panel, n = 8; right panel, n = 2) at the same point in time

Detection probability

Results from the Bayesian binomial model indicated a significant difference between detection probabilities for FS (81.20 ± 0.007%) and mono cameras (69.88 ± 0.008%). Despite this disparity, there was no difference between the 2 cameras in their probability of false negatives on the entire video (reporting a species as absent, when it is truly present), with neither detecting a shark when the other did not.

DISCUSSION

By simultaneously sampling with FS and mono cameras, we were able to demonstrate how limited FOVs may reduce the effectiveness of these optical technologies in monitoring shark populations, particularly in regions where abundances are relatively high. Our field sampling efforts revealed that catchability estimates derived from MaxN had a significant negative correlation with site abundance. These findings support previous simulation efforts, which revealed MaxN to be non-linearly related to site abundance (Schobernd et al. 2014, Campbell et al. 2015). MaxN's hyperstable relationship with site abundance is believed to be due to its basis as a maximum order statistic, whereby only the maximum count is considered. This limitation may result in estimates reaching a maximum threshold, at which they plateau due to camera saturation or issues with the spatial distribution of sharks around the cameras, while true site abundance continues to increase. For these reasons, Schobernd et al. (2014) postulated that estimates of larger predators from video data (which are often less aggregated and found in lower densities than other reef fishes) would be less influenced by issues of hyperstability. While this may be true for certain species and locations, our results do not support this hypothesis, as site density frequently exceeded the catchability threshold of mono cameras for both blacktip reef and sicklefin lemon sharks. Furthermore, whereas previous works found using MeanCount may resolve issues with hyperstability (Conn 2011, Schobernd et al. 2014, Campbell et al. 2015), we also observed a significant linear decline in catchability derived from MeanCount as site abundance increased. It is possible that the large size of our focal species coupled with densities higher than would occur naturally, as well as the presence of bait could have driven these results.

In addition to concerns surrounding catchability, mono cameras were found to have a significantly lower probability of detecting sharks than FS cameras at any given point in time. Namely, changing the cameras' FOV from mono to FS improved the probability of shark detection by nearly 12%. However, it should be noted that neither the mono (70%) nor the FS camera (81%) had a 100% estimated detection probability based on the modeled probability of occurrence, which is often assumed in ecological studies (Yoccoz et al. 2001, Kellner & Swihart 2014, Monk 2014). Failure to account for this imperfect detection can result in biased and inaccurate estimates of species distributions (Chen et al. 2013), environmental drivers of these distributions (Gu & Swihart 2004), and trends in population dynamics (Kery & Schmidt 2008, Buckland et al. 2011).

The results of this study have several implications for the use of video surveys to monitor elasmobranch populations. Indices of relative abundance, particularly for elasmobranchs, are frequently generated using zero-inflated models (i.e. delta-generalized linear

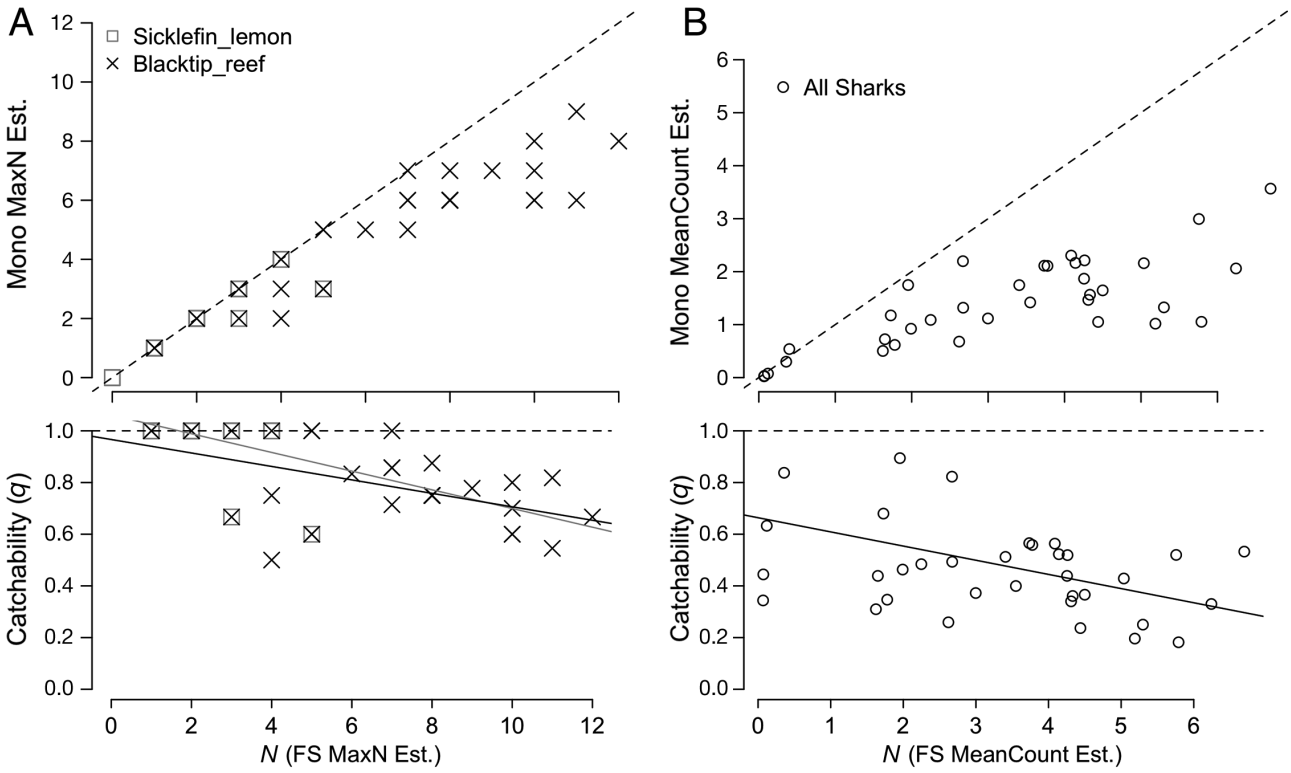

Fig. 3. (A) Relationship between site abundance (*N*, assumed to be equivalent to the full-spherical [FS] count) and estimates of MaxN from mono camera (upper panel), as well as catchability (*q*) of the mono camera (lower panel). Blacktip reef sharks *Carcharhinus melanopterus* are represented by black '×' marks, whereas sicklefin lemon sharks *Negaprion acutidens* are represented by open grey squares. Data points with both '×' and open grey squares represent both sicklefin lemon and blacktip reef sharks. Dashed lines represent the relationship that would be typically assumed for MaxN (upper panel; $y = x$), and catchability (lower panel; $q = 1.0$). Solid lines represent the fit of the linear model for each species. (B) Relationship between site abundance (assumed to be equivalent to FS count) and estimates of MeanCount from mono camera (upper panel), as well as catchability (*q*) of the mono camera (lower panel). Data are aggregated across both sicklefin lemon and blacktip reef sharks and represented by open circles. Dashed lines represent the relationship that would be typically assumed for MeanCount (upper panel; $y = x$), and catchability (lower panel; $q = 1.0$). Solid line represents the fit of the linear model

models; Bonfil 2005, Cortés 2011, Cortés et al. 2015). These types of models rely on the ability to accurately predict if a species will be present at a particular sampling location (i.e. binomial presence/absence data), as well as providing accurate counts if a species is present (i.e. Poisson presence-only data). If either component is imprecise, the resultant index of relative abundance derived from these models is also imprecise. Results from this study reveal issues surrounding both factors derived from traditional mono camera video surveys for elasmobranchs. Estimates of MaxN appear to be saturated around 6 or 7 individuals for the 2 shark species we examined. This hyperstable relationship between MaxN and true site abundance may hinder detection of changes in local population sizes through time. Imagine, for example, that a region's true site density is 12 sharks per unit area sampled by BRUVs. Given issues with saturation, as evident in this study, the estimated MaxN for this region would most likely be around 6. If this population then experience marked declines over some time period (e.g. a 50% decrease over 5 yr), estimates of MaxN would appear unchanged over this time interval, leading to the incorrect assessment that the population is relatively stable. Similarly, this saturation issue may prevent one from detecting spatial differences in relative abundance (e.g. Site 1 has a true density of 15 sharks area^{-1}, Site 2 has true density of 7 sharks area^{-1}, but both have a MaxN estimate of 7). However, it should be noted that the results of this study indicate these issues will likely only be of importance once a site density exceeds a certain threshold (i.e. 6 or 7 sharks for the focal species observed in this study). For species that occur at lower densities (and are thus likely below any threshold value), survey results from FS and mono cameras will not likely differ significantly. Although MeanCount has been shown to reduce hyperstability for teleost fishes

(Conn 2011, Schobernd et al. 2014, Campbell et al. 2015), we did not find this benefit to be true for our focal elasmobranchs. Furthermore, detection probability on any given image was relatively low for the mono camera. This low detection probability likely drove the hyperstable relationship with true site abundance by highly inflating zero counts. This in turn would also affect the binomial component (presence/absence) of any delta model approach used to create an index of relative abundance. However, the probability of a false negative for the video as a whole did not appear to be affected by the FOV of the camera. It should be noted, however, that the probability of occurrence for the entire video was not modeled, and thus catch histories of (0,0) were considered as a species being truly absent, when it is possible a species was present and simply not detected by either camera. Although this may bias our estimates of absolute detection probability, this bias would impact each gear type equally, and thus does not influence our resulting comparisons. When determining whether to use MaxN or MeanCount to enumerate elasmobranchs, researchers should also take into account species-specific considerations such as movement patterns and behaviors (e.g. slow moving species that have an affinity for the substrate may stay in front of the camera longer, and thus increase MeanCount estimates) that may influence which metric is more appropriate.

Despite the problems with mono cameras highlighted above, video surveys remain a viable tool for monitoring elasmobranch populations if limitations of restricted FOVs can be reduced or removed. By increasing the FOV to FS, we were able to greatly increase our instantaneous detection probability for elasmobranchs. Furthermore, increasing FOV reduced the effects of gear saturation at higher densities, and thus likely reduced the hyperstable relationship between counts derived from cameras and a site's true abundance. This issue may be particularly important for larger species of sharks, for which mono cameras would become saturated with relatively few individuals in the camera's FOV. Critically, these results demonstrate the influence of FOV on resulting video survey abundance estimates currently used by conservation managers to monitor elasmobranch populations. However, a major assumption of this study (as well as in previous work), is that FS cameras represent the true site abundance. FS cameras also likely experience deviations from linearity with true site abundance due to density, environmental (e.g. poor visibility), and species-specific considerations (e.g. cryptic behavior). These issues, however, should be reduced compared to standard video. Future research needs to be conducted for a variety of species, and across multiple systems to investigate the potential for regional, environmental, physical, and species-specific considerations that may influence resulting estimates. Following these efforts, it may be possible to develop a correction factor so that researchers can convert estimates of relative abundance from mono cameras to an equivalent FS estimate (e.g. with a linear model allowing for an asymptotic effect), and thus provide a method to incorporate historic data with estimates derived from emerging FS technology. FS camera technology continues to develop, including recent advances reducing the number of cameras required (i.e. BoxFish 360 VR; https://www.boxfish-research.com/products) as well as now allowing for stereo-camera length estimates of fishes (M. D. Campbell pers. obs.). As technology continues to advance, and the associated costs continue to decline, it is likely that FS video surveys will become the new norm for video surveys of elasmobranchs and teleost fishes.

Acknowledgements. The authors thank the Seeley family, the Global FinPrint Project funded by Paul G. Allen Philanthropies, and J. Hirota for funding this research. We give special thanks to the Tetiaroa Society, the Brando Hotel, and Centre de Recherches Insulaires et Observatoire de l'Environnement (CRIOBE), particularly Dr. Eric Clua, for all the help and support with field work as well as coordinating the necessary permits to operate in French Polynesia. Lastly, we thank all the interns in the Fisheries and Ecosystem Assessment Lab at Florida International University (FIU) for help with video data extraction: J. Alvarez, A. Bass, M. Castillo, D. De Mello, J. Diaz, and M. Schlegel. This is contribution #64 from the Marine Education and Research Center in the Institute for Water and Environment at FIU.

LITERATURE CITED

Bacheler NM, Schobernd CM, Schobernd ZH, Mitchell WA, Berrane DJ, Kellison GT, Reichert MJ (2013) Comparison of trap and underwater video gears for indexing reef fish presence and abundance in the southeast United States. Fish Res 143:81–88

Bond ME, Babcock EA, Pikitch EK, Abercrombie DL, Lamb NF, Chapman DD (2012) Reef sharks exhibit site-fidelity and higher relative abundance in marine reserves on the Mesoamerican Barrier Reef. PLOS ONE 7:e32983

Bonfil R (2005) Fishery stock assessment models and their application to sharks. In: Musick JA, Bonfil R (eds) Management techniques for elasmobranch fisheries. FAO Fisheries Technical Paper No. 464. FAO, Rome, p 154–181

Buckland ST, Studeny AC, Magurran AE, Newson SE (2011) Biodiversity monitoring: the relevance of detectability. In: Magurran AE, McGill B (eds) Biological diversity: frontiers in measurement and assessment. Oxford University Press, Oxford, p 25–36

Campbell MD, Pollack AG, Gledhill CT, Switzer TS, DeVries DA (2015) Comparison of relative abundance indices calculated from two methods of generating video count data. Fish Res 170:125–133

Cappo M, Harvey E, Shortis M (2007) Counting and measuring fish with baited video techniques — an overview. In: Lyle JM, Furlani DM, Buxton CD (eds) Cutting edge technologies in fish and fisheries science. Australian Society for Fish Biology Workshop Proceedings, 28–29 August 2006, Hobart, p 101–114

Chen G, Kéry M, Plattner M, Ma K, Gardner B (2013) Imperfect detection is the rule rather than the exception in plant distribution studies. J Ecol 101:183–191

Clarke C, Lea J, Ormond R (2012) Comparative abundance of reef sharks in the Western Indian Ocean. Proc 12th Int Coral Reef Symp, Cairns 13:9–13

Conn PB (2011) An evaluation and power analysis of fishery independent reef fish sampling in the Gulf of Mexico and US South Atlantic. NOAA Tech Memo NMFS-SEFSC-610. https://repository.library.noaa.gov/view/noaa/296

Cooke JG, Beddington JR (1984) The relationship between catch rates and abundance in fisheries. Math Med Biol 1: 391–405

Cortés E (2011) An overview of approaches used to assess the status of shark populations: experiences from the USA and ICCAT in the Atlantic Ocean. In: IOTC-2011-WPEB07-25. Proceedings of the 7th session of the Working Party on Ecosystems and Bycatch, 24–27 October 2011, Malé. Indian Ocean Tuna Commission, Victoria, p 1–11

Cortés E, Brooks EN, Shertzer KW (2015) Risk assessment of cartilaginous fish populations. ICES J Mar Sci 72: 1057–1068

Dapp DR, Huveneers C, Walker TI, Mandelman J, Kerstetter DW, Reina RD (2017) Using logbook data to determine the immediate mortality of blue sharks (*Prionace glauca*) and tiger sharks (*Galeocerdo cuvier*) caught in the commercial US pelagic longline fishery. Fish Bull 115:27–41

Dulvy NK, Fowler SL, Musick JA, Cavanaugh RD and others (2014) Extinction risk and conservation of the world's sharks and rays. eLife 3:e00590

Dulvy NK, Simpfendorfer CA, Davidson LN, Fordham SV, Bräutigam A, Sant G, Welch DJ (2017) Challenges and priorities in shark and ray conservation. Curr Biol 27: R565–R572

Ellis DM, DeMartini EE (1995) Evaluation of a video camera technique for indexing abundances of juvenile pink snapper, *Pristipomoides filamentosus*, and other Hawaiian insular shelf fishes. Fish Bull 93:67–77

Ferretti F, Worm B, Britten GL, Heithaus MR, Lotze HK (2010) Patterns and ecosystem consequences of shark declines in the ocean. Ecol Lett 13:1055–1071

Gallagher AJ, Serafy JE, Cooke SJ, Hammerschlag N (2014) Physiological stress response, reflex impairment, and survival of five sympatric shark species following experimental capture and release. Mar Ecol Prog Ser 496: 207–218

Gu W, Swihart RK (2004) Absent or undetected? Effects of non-detection of species occurrence on wildlife–habitat models. Biol Conserv 116:195–203

Harvey E, McLean DL, Frusher S, Haywood M, Newman S, Williams A (2013) The use of BRUVs as a tool for assessing marine fisheries and ecosystems: a review of the hurdles and potential. Fisheries Research and Development Corporation and The University of Western Australia, Perth

Kellner KF, Swihart RK (2014) Accounting for imperfect detection in ecology: a quantitative review. PLOS ONE 9: e111436

Kery M, Schmidt BR (2008) Imperfect detection and its consequences for monitoring for conservation. Community Ecol 9:207–216

Kilfoil JP, Wetherbee BM, Carlson JK, Fox DA (2017) Targeted catch-and-release of prohibited sharks: sand tigers in coastal Delaware waters. Fisheries (Bethesda, Md) 42: 281–287

Kneebone J, Chisholm J, Bernal D, Skomal G (2013) The physiological effects of capture stress, recovery, and post-release survivorship of juvenile sand tigers (*Carcharias taurus*) caught on rod and reel. Fish Res 147:103–114

Langlois TJ, Harvey ES, Fitzpatrick B, Meeuwig JJ, Shedrawi G, Watson DL (2010) Cost-efficient sampling of fish assemblages: comparison of baited video stations and diver video transects. Aquat Biol 9:155–168

Mandelman JW, Skomal GB (2009) Differential sensitivity to capture stress assessed by blood acid–base status in five carcharhinid sharks. J Comp Physiol B 179:267–277

Monk J (2014) How long should we ignore imperfect detection of species in the marine environment when modelling their distribution? Fish Fish 15:352–358

Morgan A, Carlson JK (2010) Capture time, size and hooking mortality of bottom longline-caught sharks. Fish Res 101:32–37

Plummer M (2013) rjags: Bayesian graphical models using MCMC. R package version 3

R Core Team (2015) R: a language and environment for statistical computing. R Foundation for Statistical Computing, Vienna. www.r-project.org/

Santana Garcon J, Braccini M, Langlois TJ, Newman SJ, McAuley RB, Harvey ES (2014) Calibration of pelagic stereo BRUVs and scientific longline surveys for sampling sharks. Methods Ecol Evol 5:824–833

Schobernd ZH, Bacheler NM, Conn PB (2014) Examining the utility of alternative video monitoring metrics for indexing reef fish abundance. Can J Fish Aquat Sci 71: 464–471

Stoner AW, Laurel BJ, Hurst TP (2008) Using a baited camera to assess relative abundance of juvenile Pacific cod: field and laboratory trials. J Exp Mar Biol Ecol 354: 202–211

Wells RD, Boswell KM, Cowan JH, Patterson WF (2008) Size selectivity of sampling gears targeting red snapper in the northern Gulf of Mexico. Fish Res 89:294–299

Whitmarsh SK, Fairweather PG, Huveneers C (2017) What is Big BRUVver up to? Methods and uses of baited underwater video. Rev Fish Biol Fish 27:53–73

Williams K, Rooper CN, Towler R (2010) Use of stereo camera systems for assessment of rockfish abundance in untrawlable areas and for recording pollock behavior during midwater trawls. Fish Bull 108:352–362

Willis TJ, Babcock RC (2000) A baited underwater video system for the determination of relative density of carnivorous reef fish. Mar Freshw Res 51:755–763

Worm B, Davis B, Kettemer L, Ward-Paige CA and others (2013) Global catches, exploitation rates, and rebuilding options for sharks. Mar Policy 40:194–204

Yoccoz NG, Nichols JD, Boulinier T (2001) Monitoring of biological diversity in space and time. Trends Ecol Evol 16:446–453

Appendix. Rendering full-spherical videos

Camera setting requirements for full-spherical cameras

Although both mono and full-spherical (FS) cameras were set to record at 30 frames s^{-1}, FS cameras had additional setting requirements needed to stitch FS videos correctly, including: white balance set to the temperature scale of 5500 K (outdoor), maximum ISO set to 400, sharpness set to medium, color set to 'flat', auto low light disabled, a wide angle, and a resolution of 1440p to allow for the minimum 4:3 aspect ratio.

Video stitching and synchronization

GoPro cameras split recordings into bins no larger than 4 GB, which translates to approximately 15 to 20 min of footage bin^{-1}. As such, videos taken for this study were split into multiple video files for each deployment. For both the mono and FS cameras, these separate video files were merged using MPEG Streamclip (Squared 5 srl). Although the mono camera required no further stitching, each individual camera in the F360 had to be stitched together to generate an integrated FS video. Two allied programs were used to stitch the FS videos: Kolor Autopano Giga 4.0 and Autopano Video Pro 2.0 (Kolor SAS). All 6 videos of the FS array were first imported into Autopano Video and then stitched using either the automated motion or sound syncing feature. To ensure proper synchronization, all videos were checked against a strobe flash used on deployment, with each video advanced frame-by-frame to the first frame when the flash was observed. Once synchronization was complete, all 6 videos were stitched using the calibration file provided by the F360 housing. Once the stitched file was generated, the video was then rendered using Autopano Video Pro at 2K resolution for viewing. To ensure an accurate comparison between the mono and FS cameras, each video was trimmed to the same starting point by advancing, frame-by-frame, to the start of the audio/visual synchronization point (i.e. third clap from the setter in each video).

Editorial responsibility: Peter Corkeron, Woods Hole, Massachusetts, USA

Submitted: June 14, 2017; Accepted: October 30, 2017
Proofs received from author(s): December 11, 2017